Integrated Approach for Efficient Adaptive Underdetermined DOA Estimation: Coarray LMS With Covariance Matrix Error Removal

Joel S., *Graduate Student Member, IEEE*, Shekhar Kumar Yadav, *Member, IEEE*, and Nithin V. George, *Member, IEEE*

***Abstract*—Underdetermined direction of arrival (U-DOA) estimation relies on the higher degrees of freedom provided by the difference coarray of a non-uniform linear array. The coarray domain signal is obtained by vectorizing the array covariance matrix, which is estimated using array signals from multiple snapshots. However, in low snapshot scenarios, errors arise in the covariance matrix due to non-zero off-diagonal elements in the signal and noise covariance matrices, degrading U-DOA estimation performance. This work proposes an integrated approach combining a novel covariance matrix error removal technique with the adaptive Coarray LMS and subspace-based Coarray MUSIC U-DOA estimation methods. Our method uses a matrix decomposition based approach to estimate a sparse, full-rank covariance matrix while removing low-rank residual errors caused by low snapshots. Unlike conventional methods, we treat the sparse matrix as the desired covariance matrix, addressing low-snapshot underdetermined scenarios. Additionally, we introduce a novel computationally efficient gridless approach to obtain the DOA spectrum by analyzing weights in the Fourier domain. Simulations validate the improved U-DOA estimation performance of the proposed method in low snapshot scenarios.**

***Index Terms*—Underdetermined DOA estimation, coarray LMS, coarray MUSIC, low snapshots, matrix error removal.**

I. Introduction

Direction-of-arrival (DOA) estimation involves the process of obtaining the direction of signals emitted from sources located at different spatial positions. This estimation plays an important part in various areas including modern wireless communication systems, sonar, radar and smart antenna systems. Moreover, DOA estimation serves as a critical component in various applications within smart vehicles, such as collision avoidance, autonomous driving, and advanced driver assistance systems [1], [2], [3]. Various high-resolution subspace methods [4], [5] using uniform linear arrays (ULA) have been introduced for DOA estimation. Computationally efficient adaptive DOA estimation algorithms [6], [7], [8], [9], [10], [11], [12], [13] have also been proposed recently. However, these methods can only estimate directions of fewer signals than the number of array elements. By using non-uniform linear arrays (NULAs) [14], [15], directions of more sources can be estimated with fewer array elements, which is termed as underdetermined DOA (U-DOA) estimation. The NULAs leverage the higher degrees of freedom (DOF) of their difference coarray to perform U-DOA estimation employing methods such as coarray MUSIC [14], [15], [16]. Coarray MUSIC relies on the coarray covariance matrix's Toeplitz structure, which needs a high number of temporal snapshots for this structure to manifest. Additionally, coarray MUSIC has high computational complexity as it has to perform the eigenvalue decomposition (EVD) of the coarray covariance matrix. Alternative U-DOA estimation approaches include joint sparse support recovery (JSSR) approaches, sparse recovery techniques and sparse Bayesian learning (SBL) techniques [17], [18], [19].

In our previous work [20], we proposed an efficient adaptive U-DOA estimation method using coarray signals and the least mean square (LMS) principle. The positive difference coarray was split into a reference element (zeroth position) and an auxiliary coarray. The auxiliary signal was adaptively filtered, and the error between the reference and filtered signals was minimized iteratively using LMS to compute the filter weights. These converged weights were then used to estimate the DOAs of more sources than array elements.

In scenarios where the sensing environment in the array field of view is changing quickly, we only have a low number of snapshots and it becomes very challenging to estimate the DOAs [21]. When there are only a few snapshots available, the subspace-based methods produce degraded performance due to inaccurate estimation of the signal and noise subspaces, which are calculated from the covariance matrix. For DOA estimation in low snapshot scenarios, various methods have been proposed to obtain a better estimate of the covariance matrix. A low-rank matrix denoising method was proposed for U-DOA estimation in [22] to improve the performance of coarray MUSIC in low snapshot scenarios. An algorithm based on virtual array interpolation was introduced in [23]. A sparse and parametric algorithm which relies on covariance fitting criteria and convex optimization techniques was proposed in [24]. Recently, a method was introduced for iteratively improving the sample covariance matrix with a limited number of snapshots to enhance DOA estimation in MIMO radar systems [21].

In this work, we propose efficient U-DOA estimation method for low-snapshot scenarios by integrating existing corray based algorithms with a novel low-rank residual error removal technique from the covariance matrix. Under ideal conditions, the sample covariance matrix exhibits a sparsely structured yet full-rank nature. However, in low snapshot scenarios, the error in the covariance matrix introduces low-rank residuals that can degrade the DOA estimation accuracy. We summarize the contribution of our work as follows.

Contribution 1: Our proposed method focuses on estimating a full rank sparse matrix to remove the error due to low snapshots in the covariance matrix for accurate DOA estimation. In other words, we eliminate the low-rank residual error matrix that appear due to low snapshots, effectively eliminating the undesired components. This dual capability preserving the sparse, full-rank structure of the signal covariance matrix while suppressing the low-rank error components makes our approach well-suited for low snapshot underdetermined scenarios. We propose a Principal Component Pursuit (PCP) based approach to remove covariance matrix errors in low-snapshot scenarios. The PCP algorithm [25] solves a convex optimization problem to decompose the array covariance matrix into low-rank and sparse components. In our approach, this decomposition yields a sparse matrix and a residual noise matrix from the low-snapshot covariance matrix. Instead of the conventional approach of using the low-rank matrix for denoising, we

Received 10 January 2025; revised 12 June 2025; accepted 23 July 2025. Date of publication 25 July 2025; date of current version 19 January 2026. This work was supported in part by the Department of Science and Technology, Government of India through MATRICS Scheme under Grant MTR/2022/000290 and in part by the TEOCO Chair of the Indian Institute of Technology Gandhinagar. The review of this article was coordinated by Dr. Xiaodai Dong. *(Corresponding author: Joel S.)*

Joel S. and Nithin V. George are with the Department of Electrical Engineering, Indian Institute of Technology Gandhinagar, Gandhinagar 382055, India (e-mail: joel.s@iitgn.ac.in; nithin@iitgn.ac.in).

Shekhar Kumar Yadav was with the Department of Electrical Engineering, Indian Institute of Technology Gandhinagar, Gandhinagar 382055, India. He is now with Audio Information Processing Lab, Technical University of Munich (TUM), 80333 München, Germany (e-mail: yadav_shekhar@iitgn.ac.in).

Digital Object Identifier 10.1109/TVT.2025.3592938

utilize the sparse matrix as the desired covariance matrix, eliminating the low-rank residual matrix that contains errors from low snapshots. The proposed algorithms have better DOA estimation in lower snapshot scenarios compared to the existing baseline algorithms.

Contribution 2: Another key contribution of our proposed algorithm is the development of a novel and computationally efficient off-grid method for obtaining the spatial spectrum using coarray weights through a Fourier domain approach.

Notations: $(.)^*$, $(.)^{\mathrm{T}}$, $(.)^{\mathrm{H}}$ refer to the conjugate, transpose and the conjugate transpose operator, respectively. $\otimes$ denotes the Kronecker product and $\mathbb{C}$ refers to the set of complex numbers. $\mathbb{E}[.]$ is the mathematical expectation operator.

II. Array Signal Model

We examine a scenario in which uncorrelated signals originating from Q narrowband sources arrive at a nested linear array [14] comprising of M sensors. Despite opting for a nested array configuration, the U-DOA estimation technique introduced in this paper is applicable to any non-uniform linear array (NULA) that has a contiguous uniform difference coarray without any holes. It is assumed that the sources are situated in the far field of the array. The signal received by the M Sensors of the array at the l^{th} snapshot is expressed as

$$\mathbf{u}(l) = \sum\nolimits_{q=1}^{Q} \mathbf{a}(\tilde{\theta}_q) x_q(l) + \boldsymbol{\beta}(l) = \mathbf{A}\mathbf{x}(l) + \boldsymbol{\beta}(l). \tag{1}$$

Here, $\mathbf{a}(\tilde{\theta}_q) = [e^{j2\pi\tilde{\theta}_q m_1}, e^{j2\pi\tilde{\theta}_q m_2}, \ldots, e^{j2\pi\tilde{\theta}_q m_M}]^{\mathrm{T}}$ denotes the steering vector associated with the q^{th} source, where $\{m_1, m_2, \ldots, m_M\}$ denotes the positions of the M sensors. $\tilde{\theta}_q$ represents the normalized DOA, defined as $\tilde{\theta}_q = (d/\Delta)\sin\theta_q$, where d denotes the smallest spacing between the sensor, Δ denotes the wavelength of the signals, and θ_q represents the actual DOA of the q^{th} source. For a linear array, the range of θ_q spans from $-\pi/2$ to $\pi/2$, and given our selection of $d = \Delta/2$, the range of $\tilde{\theta}_q$ falls within $[-0.5, 0.5]$. Moreover, in equation (1), $\mathbf{x}(l) = [x_1(l), x_2(l), \ldots, x_Q(l)]^{\mathrm{T}}$ represents the vector containing the amplitudes of the Q signals. $\mathbf{A} = [\mathbf{a}(\tilde{\theta}_q), \mathbf{a}(\tilde{\theta}_2), \ldots, \mathbf{a}(\tilde{\theta}_Q)] \in \mathbb{C}^{M\times Q}$ is referred to as the steering matrix, and $\boldsymbol{\beta}(l)$ represents the sensor noise, which is considered to be uncorrelated with the source signals. The objective of this work is to estimate the unknown DOAs, $\tilde{\theta}_q$, of the Q sources in the underdetermined scenario ($Q > M$) with a low number of snapshots.

III. Proposed Method

A. Integrated Approach: Existing Coarray Based Methods Integrated With the Proposed Covariance Matrix Error Removal

Underdetermined DOA estimation methods, like the adaptive Coarray LMS [20] and subspace-based algorithms, like Coarray MUSIC [14] uses covariance matrix. Therefore, accurate covariance matrix estimation is crucial for DOA estimation for such existing methods. The covariance matrix is expressed as

$$\mathbf{P}_u = \mathbb{E}\left[\mathbf{u}(l)\mathbf{u}^{\mathrm{H}}(l)\right] = \mathbf{A}\mathbf{P}_x\mathbf{A}^{\mathrm{H}} + \rho^2\mathbf{I}_M, \tag{2}$$

where $\mathbf{P}_x$ is a diagonal matrix containing the powers of the source signals and $\mathbf{I}_M$ is an identity matrix of dimension $M \times M$ with ρ^2 being the noise power in each sensor. However, sample covariance matrix $\hat{\mathbf{P}}_u = \frac{1}{L}\sum_{l=1}^{L}\mathbf{u}(l)\mathbf{u}^{\mathrm{H}}(l)$ is used instead of $\mathbf{P}_u$ in practical scenarios using L snapshots. But, in scenarios where only a few snapshots are available, the sample covariance matrix is not able to accurately represent the actual array covariance matrix. So, there is

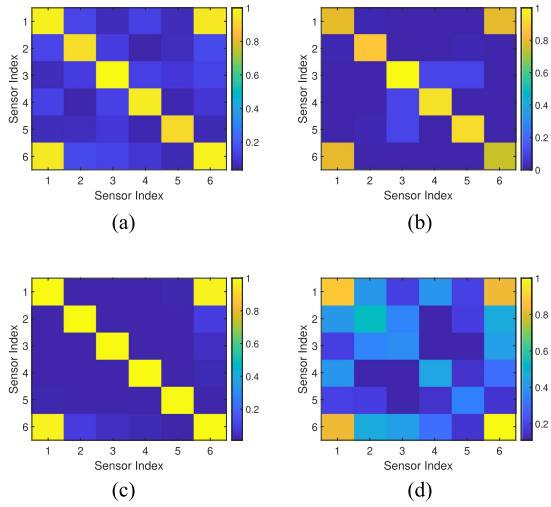

Fig. 1. (a) Sample, (b) estimated and (c) ideal covariance matrices along with the (d) error matrix for a nested array configuration ($M_1 = M_2 = 3$) for SNR $= 20$ dB and number of snapshots $= 100$. The estimated covariance matrix is sparser and closer to the ideal covariance matrix than the sample covariance matrix. (a) Sample covariance matrix. (b) Estimated covariance matrix from the proposed method. (c) Ideal covariance matrix. (d) Error matrix.

an error in the sample covariance matrix which causes degradation in DOA estimation performance in low snapshot scenarios. The error mainly appears as the non-zero cross-correlation non-diagonal terms in the signal covariance matrix $\mathbf{P}_x$ and the noise covariance matrix $\rho^2\mathbf{I}_M$. This is because, in the case of low snapshots, the uncorrelated source signals have some correlation, and as such, the signal covariance matrix is no longer diagonal. The same happens to the noise covariance matrix. Therefore, the sample covariance matrix under a low snapshot scenario can be expressed as

$$\hat{\mathbf{P}}_u = \mathbf{P}_u + \mathbf{E} = \mathbf{A}\left(\mathbf{P}_x + \mathbf{E}_x\right)\mathbf{A}^{\mathrm{H}} + (\rho^2\mathbf{I}_M + \mathbf{E}_\beta), \tag{3}$$

where $\mathbf{E}$ is the error in the sample covariance matrix that has been introduced due to the error ($\mathbf{E}_x$) in the estimation of the signal covariance matrix and the error ($\mathbf{E}_\beta$) in the estimation of the noise covariance matrix. To remove the effect of error in the covariance matrix estimation, we propose a new algorithm for any DOA estimation method that uses the covariance matrix, such as the adaptive and the subspace-based algorithms. The proposed Matrix Error Removal (MER) method uses the PCP matrix decomposition technique and decomposes the sample covariance matrix into a sparse matrix ($\mathbf{G}$) and a residual error matrix ($\mathbf{F}$). The justification for this is that, in (3), the ideal covariance matrix $\mathbf{P}_u$ is sparse. The sparse nature of the ideal covariance matrix can be seen in Fig. 1(c), where most values of the covariance matrix are zero or close to zero. Thus, the sparse component ($\mathbf{G}$) of the proposed decomposition would be a better estimate of the ideal covariance matrix $\mathbf{P}_u$ than the sample covariance matrix. To obtain $\mathbf{G}$ and $\mathbf{F}$, we create a constrained optimization problem

$$\min \|\mathbf{F}\|_* + \lambda\|\mathbf{G}\|_1 \quad \text{s.t.} \quad \|\hat{\mathbf{P}}_u - \mathbf{F} - \mathbf{G}\|_F^2 < \epsilon, \tag{4}$$

where $\|\mathbf{F}\|_*$ denotes the nuclear norm (sum of singular values) of matrix $\mathbf{F}$, $\|\mathbf{G}\|_1$ denotes the ℓ_1 norm (sum of absolute values) of matrix $\mathbf{G}$. λ is a regularisation parameter that regularizes between minimizing $\|\mathbf{F}\|_*$ and minimizing $\|\mathbf{G}\|_1$. We minimize the ℓ_1-norm of $\mathbf{G}$ to encourage sparsity to better estimate $\mathbf{P}_u$. $\|\hat{\mathbf{P}}_u - \mathbf{F} - \mathbf{G}\|_F^2$ denotes the Frobenius norm squared of matrix $(\hat{\mathbf{P}}_u - \mathbf{F} - \mathbf{G})$. The constraint ensures that the sum of the decomposed components $(\mathbf{F} + \mathbf{G})$ is as close as possible to $\hat{\mathbf{P}}_u$

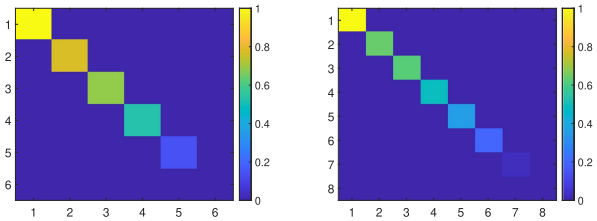

Fig. 2. A matrix whose diagonals are the singular values of the error matrix for two different nested array configurations for SNR = 20 dB and number of snapshots (L) = 100. (a) $M_1 = M_2 = 3$. (b) $M_1 = 3, M_2 = 5$.

(ϵ is a small user-defined parameter that controls the permissible margin of error and penalizing deviations from the error). The motivation for minimizing the nuclear norm of $\mathbf{F}$ is provided in Fig. 2. The figure shows the singular values of the error matrix (the error matrix is the error between the ideal covariance and sample covariance matrix). From the figure, we can see that the error matrix is a low-rank matrix, which motivates us to minimize the nuclear norm of $\mathbf{F}$ to estimate the error matrix accurately.

The optimization problem in (4) can be written in an unconstrained form using the Lagrange multiplier principle with the minimization of the following augmented Lagrangian cost function

$$\mathcal{L}_\gamma(\mathbf{F},\mathbf{G},\boldsymbol{\mathcal{Y}}) = \|\mathbf{F}\|_* + \lambda\|\mathbf{G}\|_1 + \langle \boldsymbol{\mathcal{Y}}, \hat{\mathbf{P}}_u - \mathbf{F} - \mathbf{G}\rangle + \frac{\gamma}{2}\|\hat{\mathbf{P}}_u - \mathbf{F} - \mathbf{G}\|_F^2, \tag{5}$$

where $\boldsymbol{\mathcal{Y}}$ is the Lagrange multiplier and γ is the penalty parameter. $\langle \boldsymbol{\mathcal{Y}}, \hat{\mathbf{P}}_u - \mathbf{F} - \mathbf{G}\rangle$ denotes the inner product between matrices $\boldsymbol{\mathcal{Y}}$ and $(\hat{\mathbf{P}}_u - \mathbf{F} - \mathbf{G})$.

1) Update Process for $\mathbf{F}$*:* We now update $\mathbf{F}$ by minimization the augmented Lagrangian with respect to $\mathbf{F}$, while keeping $\mathbf{G}$ and $\boldsymbol{\mathcal{Y}}$ fixed. That is, the update equation for $\mathbf{F}$ is written as follows

$$\mathbf{F}^{k+1} = \text{argmin}_{\mathbf{F}}\, \mathcal{L}_\gamma\left(\mathbf{F}, \mathbf{G}^k, \boldsymbol{\mathcal{Y}}^k\right). \tag{6}$$

We solve this by performing singular value thresholding (SVT) or using singular value decomposition (SVD) with a threshold and a reconstruction operation as follows:

- *SVT is implemented as:* If $\mathbf{F} = \mathbf{U}\boldsymbol{\Sigma}\mathbf{V}^{\mathrm{T}}$ is the SVD of $\mathbf{F}$, where $\mathbf{U}$ and $\mathbf{V}$ are orthogonal matrices and Σ is a diagonal matrix containing the singular values of $\mathbf{F}$, then the nuclear norm of $\mathbf{F}$ is the sum of the singular values, and thresholding those singular values leads to an update. Let σ_i denote the i^{th} singular value of $\mathbf{F}$, then the thresholded singular values are given by

$$\sigma_i^{k+1} = \text{sign}\left(\sigma_i^k\right) \cdot \max\left(\left|\sigma_i^k\right| - \frac{1}{\gamma}, 0\right), \tag{7}$$

  where σ_i^k are the singular values of the previous estimate $\mathbf{F}^k$.
- *Reconstruct* $\mathbf{F}^{k+1}$*:* After obtaining the thresholded singular values, we reconstruct the updated matrix $\mathbf{F}^{k+1}$ using the thresholded singular values as

$$\mathbf{F}^{k+1} = \mathbf{U}\boldsymbol{\Sigma}^{k+1}\mathbf{V}^{\mathrm{T}}. \tag{8}$$

  This new matrix $\mathbf{F}^{k+1}$ is a solution that minimizes the augmented Lagrangian function with respect to $\mathbf{F}$ while keeping $\mathbf{G}$ and $\boldsymbol{\mathcal{Y}}$ fixed.

By updating $\mathbf{F}$ in this manner, we progress towards a solution that minimizes the overall objective function.

2) Update Process for $\mathbf{G}$*:* Similarly, to update $\mathbf{G}$, we minimize the augmented Lagrangian with respect to $\mathbf{G}$, while keeping $\mathbf{F}$ and $\boldsymbol{\mathcal{Y}}$ fixed as

$$\mathbf{G}^{k+1} = \text{argmin}_{\mathbf{G}}\, \mathcal{L}_\gamma\left(\mathbf{F}^{k+1}, \mathbf{G}, \boldsymbol{\mathcal{Y}}^k\right). \tag{9}$$

We solve this by using a soft-thresholding problem. Soft-thresholding shrinks or thresholds individual elements of a matrix towards zero, resulting in sparse solutions. Given a matrix $\mathbf{X}$, soft-thresholding is defined as

$$\text{soft-threshold}(\mathbf{X}, \delta) = \text{sign}(\mathbf{X}) \cdot \max\left(|\mathbf{X}| - \delta, 0\right), \tag{10}$$

where $\text{sign}(\mathbf{X})$ denotes the sign function applied element-wise to $\mathbf{X}$, and δ is a non-negative threshold parameter. To obtain $\mathbf{G}^{k+1}$, we apply the soft-thresholding operation element-wise to the matrix $(\hat{\mathbf{P}}_u - \mathbf{F}^{k+1} - \boldsymbol{\mathcal{Y}}^k/\gamma)$ as

$$\mathbf{G}^{k+1} = \text{soft-threshold}\left(\hat{\mathbf{P}}_u - \mathbf{F}^{k+1} - \boldsymbol{\mathcal{Y}}^k/\gamma, \lambda/\gamma\right). \tag{11}$$

This operation shrinks the elements of $\hat{\mathbf{P}}_u - \mathbf{F}^{k+1} - \boldsymbol{\mathcal{Y}}^k/\gamma$ towards zero, effectively encouraging sparsity in the matrix $\mathbf{G}^{k+1}$. By updating $\mathbf{G}$ in this manner, we once again progress towards a solution that minimizes the overall objective function. This process is then repeated iteratively until convergence, with updated $\mathbf{F}$ used in every iteration.

3) Update Process for $\boldsymbol{\mathcal{Y}}$*:* We update the Lagrange multiplier using the following equation

$$\boldsymbol{\mathcal{Y}}^{k+1} = \boldsymbol{\mathcal{Y}}^k + \gamma\left(\hat{\mathbf{P}}_u - \mathbf{F}^{k+1} - \mathbf{G}^{k+1}\right). \tag{12}$$

The Lagrange multiplier $\boldsymbol{\mathcal{Y}}$ is updated to enforce the constraint $\hat{\mathbf{P}}_u = \mathbf{F} + \mathbf{G}$. This update ensures that the difference between $\hat{\mathbf{P}}_u$ and the current estimates of $\mathbf{F}$ and $\mathbf{G}$ is consistent with the Lagrange multiplier. In this first step, we calculate the residual matrix as

$$\mathbf{R}^{k+1} = \hat{\mathbf{P}}_u - \mathbf{F}^{k+1} - \mathbf{G}^{k+1}. \tag{13}$$

Then, we update the Lagrange multiplier $\boldsymbol{\mathcal{Y}}$ using the following formula

$$\boldsymbol{\mathcal{Y}}^{k+1} = \boldsymbol{\mathcal{Y}}^k + \gamma\mathbf{R}^{k+1}. \tag{14}$$

This update increases $\boldsymbol{\mathcal{Y}}$ in the direction of the residual matrix $\mathbf{R}^{k+1}$ scaled by the penalty parameter γ. By adjusting $\boldsymbol{\mathcal{Y}}$, the algorithm encourages the estimates of $\mathbf{F}$ and $\mathbf{G}$ to move closer to satisfying the equality constraint $\hat{\mathbf{P}}_u = \mathbf{F} + \mathbf{G}$.

This step ensures that the Lagrange multiplier $\boldsymbol{\mathcal{Y}}$ evolves appropriately throughout the optimization process to maintain consistency with the current estimates of $\mathbf{F}$ and $\mathbf{G}$. For every iteration, we keep checking the convergence criteria. If the convergence criteria are not met, we keep repeating the entire procedure. The block diagram of the proposed algorithm to estimate the covariance matrix for low snapshots scenario integrated with Coarray LMS is presented in Fig. 3. After convergence, the matrix $\mathbf{G}$ is the estimated error removed covariance matrix that can be used for any DOA estimation algorithm that uses the covariance matrix. In coarray LMS, the estimated covariance matrix is used to obtain the coarray signal that is used to update the auxiliary coarray weights to estimate the U-DOAs. In coarray MUSIC, the estimated covariance matrix is used to obtain the coarray noise subspace through the coarray signal to obtain the U-DOA spectrum.

B. Coarray Fourier Domain Off-Grid DOA Estimation

In this section, we present a novel computationally efficient method in the Fourier domain for obtaining the DOA spatial spectrum from the adaptive coarray weight vector $\mathbf{w}_f$. The null spectrum of the coarray

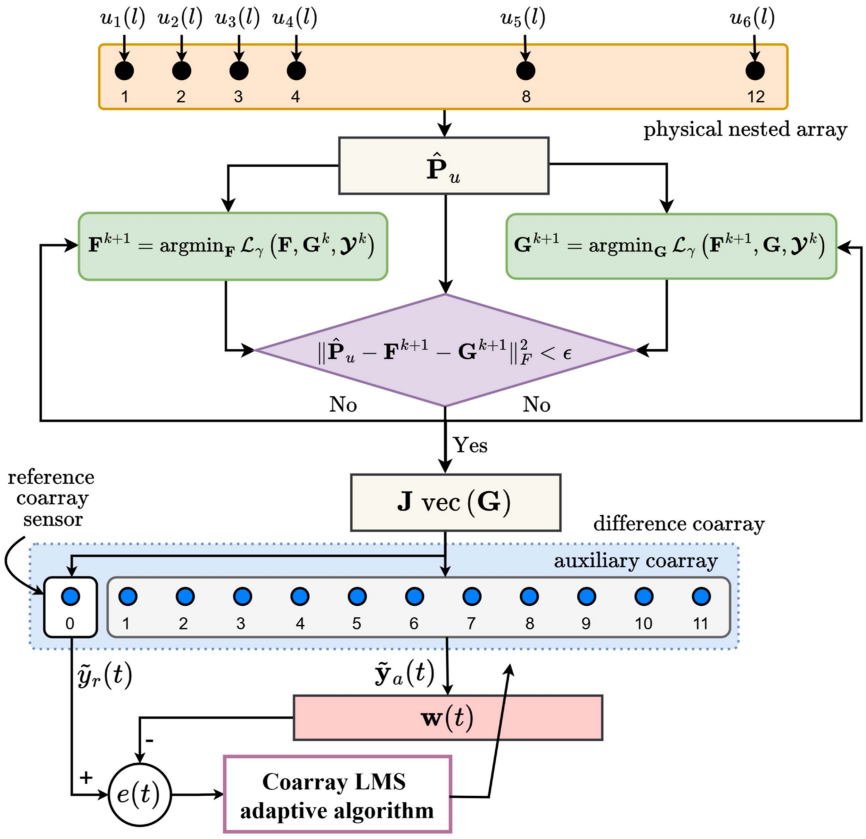

Fig. 3. Block diagram depicting the integration of the proposed matrix error removal (MER) method with the Coarray LMS adaptive algorithm.

LMS [20] spatial spectrum $\mathcal{S}(\tilde{\theta})$ is denoted as $h(\tilde{\theta}) = \mathbf{w}_f^{\mathrm{H}} \tilde{\mathbf{a}}_f(\tilde{\theta})$, where $\mathbf{w}_f = \begin{bmatrix} 1 \\ -\mathbf{w} \end{bmatrix}$, $\tilde{\mathbf{a}}_f(\tilde{\theta}) = \begin{bmatrix} 1 \\ \tilde{\mathbf{a}}_c^+(\tilde{\theta}) \end{bmatrix}$ and $\tilde{\mathbf{a}}_c^+(\tilde{\theta})$ is the auxiliary coarray steering vector of the positive part of the difference coarray as shown in Fig. 3. This null spectrum exhibits periodicity in θ with a period of 2π. This periodic behaviour arises from the formulation of the steering vector $\tilde{\mathbf{a}}_f(\tilde{\theta})$. Consequently, h can be represented as a Fourier series, expressed as:

$$h(\omega) = \sum_{m=-\infty}^{\infty} H_m e^{jm\omega}, \tag{15}$$

where H_m are the Fourier series coefficients expressed as

$$H_m = \frac{1}{2\pi} \int_{-\pi}^{\pi} h(\omega)\, e^{-jm\omega} d\omega. \tag{16}$$

Comparing $h(\omega)$ with $h(\tilde{\theta})$ and noting that $\tilde{\theta} = \sin\theta/2$, it can be observed that $\omega = \pi \sin\theta$ and $\{H_m\}_{m=0}^{(M_2(M_1+1)-1)} = [\mathbf{w}_f]_{m=1}^{M_2(M_1+1)}$. Therefore, the truncation of Fourier series expansion in (15) is given by

$$h(\omega) = \sum_{m=0}^{(M_2(M_1+1)-1)} [\mathbf{w}_f]_{m+1} e^{jm\omega}, \tag{17}$$

Thus, the null spectrum $\mathcal{S}(\tilde{\theta})$ can be derived through the discrete Fourier transform (DFT) of the coarray weight vector $\mathbf{w}_f$. This DFT computation can efficiently be performed using the fast Fourier transform (FFT) method. To enhance the resolution of the null spectrum, we augment the coarray weight vector by padding zeros, modifying the expression in (17) as

$$h(n) = \sum_{m=0}^{M_{\mathrm{F}}} [\mathbf{w}_f]_{m+1} e^{j\frac{2\pi}{M_{\mathrm{F}}+1} nm}, \quad n = 0, 1, \ldots, M_{\mathrm{F}}, \tag{18}$$

where M_{F} is significantly greater than $(M_2(M_1+1)-1)$. After acquiring the $(M_{\mathrm{F}}+1)$ point FFT coefficients denoted as $h(n)$, we compute the Fourier domain spectrum as

$$F(n) = 1/h(n), \quad n = 0, 1, \ldots, M_{\mathrm{F}}. \tag{19}$$

To determine the DOAs, we transition from the Fourier domain spectrum to the spatial spectrum. This transition from the Fourier domain FFT points to the spatial spectrum domain is achieved as $\tilde{\theta} = (\frac{n - 0.5 * M_{\mathrm{F}}}{M_{\mathrm{F}}})$, where n ranges from 0 to M_{F}, representing the FFT point index (with a total of $M_{\mathrm{F}}+1$ FFT points), and $\tilde{\theta}$ is mapped within the interval $[-0.5, 0.5]$. Following this mapping, the peaks observed in the spatial spectrum align with the DOAs of the signals. The proposed Fourier domain (FD) spectrum, along with coarray LMS and the proposed matrix error removal algorithm, is referred to as Coarray FD-LMS-MER. The pseudocode of Coarray FD-LMS-MER is shown in Algorithm 1.

In Table I, we show the computational complexity of all the algorithms. The number of FFT points used for coarray FD-LMS and coarray FD-LMS-MER is denoted by $M_F + 1$ and the computations is shown for 1 iteration. For Coarray MUSIC and coarray MUSIC-MER, G and N are the number of grid points and number of noise subspace eigen vectors, respectively. A comparison of computational complexity for the same number of grid points in the grid search method and an equal number of FFT points in our proposed off-grid Fourier Domain (FD) approach is provided. Let $G = 10000$ be the number of angular grid points for grid search approaches and $M_F = 10000$ be the number of FFT points for our proposed off grid FD approach. The computational complexity of grid search is $M_f \times G = 120000$ and for FD approach, the computational complexity is $(\frac{M_{\mathrm{F}}+1}{2})\log_2(M_{\mathrm{F}}+1) = 66439$. The computational savings for our FD approach is approximately 44.63%.

Algorithm 1: Coarray FD-LMS-MER.

Input: Array signal $\mathbf{u}(l)\ \forall\ l \in \{1, 2, \ldots, L\}$
Initialization: $\mathbf{w}(0) = \mathbf{0}$, μ (step size), $\hat{\mathbf{P}}_u(0) = \mathbf{0}$, λ, γ.
for $t = 1 : \mathcal{T}$, **do** ($\mathcal{T}$ is the number of iterations)
$\hat{\mathbf{P}}_u(t) = \hat{\mathbf{P}}_u(t-1) + \sum_{t=1+(L/\mathcal{T})(t-1)}^{(L/\mathcal{T})+(L/\mathcal{T})(t-1)} \mathbf{u}(t)\mathbf{u}^{\mathrm{H}}(t)$
$\hat{\mathbf{P}}_u(t) = \hat{\mathbf{P}}_u(t)/(Lt/\mathcal{T})$
for $k = 1 : \mathcal{K}$, **do**
$\mathbf{F}^{k+1} = \mathrm{argmin}_{\mathbf{F}}\ \mathcal{L}_\gamma(\mathbf{F}, \mathbf{G}^k, \boldsymbol{\mathcal{Y}}^k)$
$\mathbf{G}^{k+1} = \mathrm{argmin}_{\mathbf{G}}\ \mathcal{L}_\gamma(\mathbf{F}^{k+1}, \mathbf{G}, \boldsymbol{\mathcal{Y}}^k)$
$\mathbf{R}^{k+1} = \hat{\mathbf{P}}_u - \mathbf{F}^{k+1} - \mathbf{G}^{k+1}$
$\boldsymbol{\mathcal{Y}}^{k+1} = \boldsymbol{\mathcal{Y}}^k + \gamma\mathbf{R}^{k+1}$
if $\|\hat{\mathbf{P}}_u - \mathbf{F}^{k+1} - \mathbf{G}^{k+1}\|_F^2 < \epsilon$
break
end
$\tilde{\mathbf{y}}(t) = \mathbf{J}\ \mathrm{vec}(\mathbf{G}^{k+1}) = [\tilde{\mathbf{y}}_a^*(t), \tilde{y}_r(t), \tilde{\mathbf{y}}_a(t)]^{\mathrm{T}}$
$e(t) = \tilde{y}_r(t) - \mathbf{w}^{\mathrm{H}}(t)\tilde{\mathbf{y}}_a(t)$
coarray LMS weight update
$\mathbf{w}(t+1) = \mathbf{w}(t) + \mu e^*(t)\tilde{\mathbf{y}}_a(t)$
end
coarray LMS spatial spectrum: $\mathcal{S}(\tilde{\theta}) = \frac{1}{h(\tilde{\theta})} = \frac{1}{|\mathbf{w}_f^{\mathrm{H}}\tilde{\mathbf{a}}_f(\tilde{\theta})|}$
coarray FD-LMS spectrum: $F(n) = \frac{1}{h(n)}$
DOA estimates: (i) peaks of $\mathcal{S}(\tilde{\theta})$, (ii) peaks of $F(n)$

TABLE I
COMPUTATIONAL COMPLEXITY

Algorithm	Complexity
coarray FD-LMS	$\mathcal{O}\left(M^2L + 2M_f + 1 + (\frac{M_{\mathrm{F}}+1}{2})\log_2(M_{\mathrm{F}}+1)\right)$
coarray MUSIC	$\mathcal{O}\left(M^2L + (M_f+1)^3 + N(M_f+1)G\right)$
coarray FD-LMS-MER	$\mathcal{O}\left(M^2L + 2M_f + 1 + \mathcal{K}(M_f+1)^3 + (\frac{M_{\mathrm{F}}+1}{2})\log_2(M_{\mathrm{F}}+1)\right)$
coarray MUSIC-MER	$\mathcal{O}\left(M^2L + (\mathcal{K}+1)(M_f+1)^3 + N(M_f+1)G\right)$

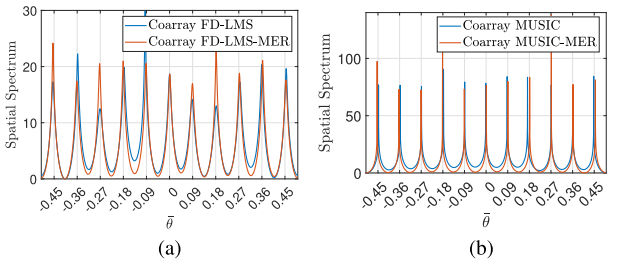

Fig. 4. (a) Fourier Domain spatial spectrum of coarray FD-LMS and coarray FD-LMS-MER with $\mu = 0.001$ and $\mathcal{T} = 6$ (b) Spatial spectrum of coarray MUSIC and coarray MUSIC-MER, for SNR $= 20$ dB, $Q = 11$, $L = 150$.

IV. SIMULATIONS AND DISCUSSIONS

In this section, we perform underdetermined DOA estimation using our proposed method to highlight its effectiveness. We use a nested array [14] of $M = 6$ physical array elements, with $M_1 = 3$ and $M_2 = 3$. The Q sources are assumed to be uncorrelated, each with equal power, and are distributed uniformly across the range from $\tilde{\theta}_1 = -0.45$ to $\tilde{\theta}_Q = 0.45$. In Fig. 4(a), the spatial spectrum obtained using the proposed Coarray FD-LMS-MER method is presented and compared with the Coarray FD-LMS method. Similarly, Fig. 4(b) shows the spatial spectrum derived using the proposed Coarray MUSIC-MER and compared with the spatial spectrum of Coarray MUSIC. All spatial spectrum are plotted for $Q = 11$ sources at an SNR of 20 dB. The number of snapshots is kept at $L = 150$. The number of grid points

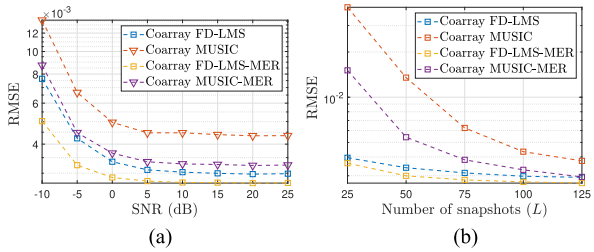

Fig. 5. Variation of RMSE of the proposed Coarray FD-LMS-MER and Coarray MUSIC-MER in comparison with their respective baseline algorithms for varying (a) SNR and (b) number of snapshots (L) for $Q = 11$. (a) Number of snapshots $L = 100$. (b) SNR $= 20$ dB.

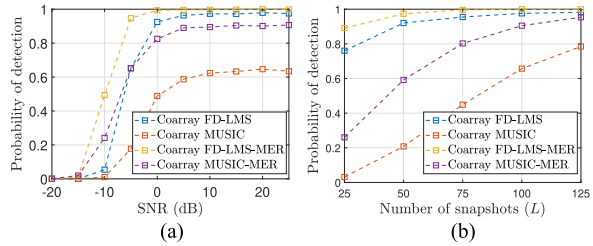

Fig. 6. Variation of PD of Coarray FD-LMS-MER and Coarray MUSIC-MER in comparison with other algorithms for $Q = 11$ with respect to (a) SNR, (b) number of snapshots (L). (a) Number of snapshots $L = 100$. (b) SNR $=$ 20 dB.

and the number of FFT points were set to 10,000. As observed in Fig. 4(a) and (b), all the algorithms identified the necessary peaks. However, the peaks obtained by the proposed Coarray FD-LMS-MER and Coarray MUSIC-MER are closer to the true DOA locations compared to the baseline algorithms. This enhanced accuracy at low snaphots is further analyzed and validated through RMSE plots. In all the subsequent simulations, we run our proposed algorithm till the condition $\|\mathbf{R}^{k+1}\|_F^2 = \|\hat{\mathbf{P}}_u - \mathbf{F}^{k+1} - \mathbf{G}^{k+1}\|_F^2 < 10^{-5}$ is satisfied or till $\mathcal{K} = 1000$ iterations. The other parameters of the proposed algorithm are $\lambda = 0.4082$ and $\gamma = 0.4$. To evaluate the performance of the proposed algorithms, we analyse the RMSE (root-mean-squared-error) of normalized DOA estimation for different SNRs and number of snapshots. The RMSE is calculated as RMSE $= \sqrt{\frac{1}{JQ}(\tilde{\theta}_{q,j} - \hat{\tilde{\theta}}_{q,j})}$, where $\tilde{\theta}_{q,j}$ and $\hat{\tilde{\theta}}_{q,j}$ are the actual and estimated DOA of the q^{th} source at the j^{th} Monte Carlo (MC) trial, respectively. J is the total MC trials and it is set to $J = 2000$. Fig. 5 show the RMSE performances (normalized DOA) of the proposed Coarray FD-LMS-MER and Coarray MUSIC-MER for different SNRs and number of snapshots, and they are compared with the baseline Coarray FD-LMS and Coarray MUSIC algorithms. The number of sources is $Q = 11$, and the number of snapshots for plots with varying SNR in Fig. 5(a) is kept at $L = 100$. The figures show the proposed algorithms outperform their respective baseline counterparts. Coarray FD-LMS-MER is outperforming all the algorithms, including the subspace-based Coarray MUSIC and Coarray MUSIC-MER algorithms. An important performance measure for DOA estimation methods is the probability of detection. It is defined as PD $= \frac{J_s}{J}$, where J_s is the number of successful trials among the J total trials. A DOA estimation trail is considered to be successful if the DOA peaks of all the Q sources are detected and $|\tilde{\theta}_{q,j} - \hat{\tilde{\theta}}_{q,j}| < 0.0087$ for all Q sources. Fig. 6 show the PD performance of the proposed Coarray FD-LMS-MER and Coarray MUSIC-MER, along with the baselines

for $Q = 11$. From the figures, the proposed algorithms have a higher probability of detecting all the sources than their baselines for varying SNRs and number of snapshots. The Coarray FD LMS-MER and Coarray MUSIC-MER algorithms have a limitation of having higher computational complexity compared to the baseline algorithms due to covariance error removal but offer improved DOA estimation accuracy in low snapshot scenarios.

V. Conclusion

In low snapshot scenarios, DOA estimation is impacted by covariance matrix errors. We propose a method combining matrix error removal with underdetermined DOA estimation, using covariance matrix decomposition into sparse and low-rank components. An augmented Lagrangian cost function minimizes these matrices iteratively, removing errors from the covariance matrix. The corrected matrix is then used with the coarray LMS and coarray MUSIC algorithms for U-DOA estimation. Additionally, we introduce a computationally efficient gridless Fourier domain-based coarray spatial spectrum technique. The effectiveness of our integrated approach is demonstrated through various simulations.

References

[1] W. Liu, M. Haardt, M. S. Greco, C. F. Mecklenbräuker, and P. Willett, "Twenty-five years of sensor array and multichannel signal processing: A review of progress to date and potential research directions," *IEEE Signal Process. Mag.*, vol. 40, no. 4, pp. 80–91, Jun. 2023.

[2] X. Dong, X. Zhang, J. Zhao, M. Sun, and Q. Wu, "Multi-maneuvering sources DOA tracking with improved interactive multi-model multi-bernoulli filter for acoustic vector sensor (AVS) array," *IEEE Trans. Veh. Technol.*, vol. 70, no. 8, pp. 7825–7838, Aug. 2021.

[3] Z. Guo, X. Wang, and X. Zeng, "Unambiguous direction-of-arrival estimation for improved scanning efficiency in subarray-based hybrid array," *IEEE Trans. Veh. Technol.*, vol. 70, no. 8, pp. 7966–7979, Aug. 2021.

[4] R. Schmidt, "Multiple emitter location and signal parameter estimation," *IEEE Trans. Antennas Propag.*, vol. TAP-34, no. 3, pp. 276–280, Mar. 1986.

[5] R. Roy and T. Kailath, "ESPRIT-estimation of signal parameters via rotational invariance techniques," *IEEE Trans. Acoust., Speech, Signal Process.*, vol. 37, no. 7, pp. 984–995, Jul. 1989.

[6] H. Zeng, Z. Ahmad, J. Zhou, Q. Wang, and Y. Wang, "DOA estimation algorithm based on adaptive filtering in spatial domain," *China Commun.*, vol. 13, no. 12, pp. 49–58, 2016.

[7] B. Jalal, X. Yang, X. Wu, T. Long, and T. K. Sarkar, "Efficient direction-of-arrival estimation method based on variable-step-size LMS algorithm," *IEEE Antennas Wireless Propag. Lett.*, vol. 18, no. 8, pp. 1576–1580, Aug. 2019.

[8] C. Liu and H. Zhao, "Efficient DOA estimation method using bias-compensated adaptive filtering," *IEEE Trans. Veh. Technol.*, vol. 69, no. 11, pp. 13087–13097, Nov. 2020.

[9] H. Zhao, W. Luo, Y. Liu, and C. Wang, "A variable step size gradient-descent TLS algorithm for efficient DOA estimation," *IEEE Trans. Circuits Syst. II, Exp. Briefs*, vol. 69, no. 12, pp. 5144–5148, Dec. 2022.

[10] B. Jalal, O. Elnahas, X. Xu, Z. Quan, and P. Zhang, "Robust DOA estimation using VSS-LMS with low-rank matrix approximation," *IEEE Trans. Aerosp. Electron. Syst.*, vol. 59, no. 3, pp. 2967–2978, Jun. 2023.

[11] S. Joel, K. Kumar, and N. V. George, "Robust DOA estimation based on an exponential hyperbolic cosine adaptive algorithm," *IEEE Sens. Lett.*, vol. 7, no. 5, May 2023, Art. no. 7001904.

[12] S. Joel, S. K. Yadav, and N. V. George, "Adaptive low-rank DOA estimation using complex Kronecker product decomposition," *IEEE Trans. Veh. Technol.*, vol. 73, no. 7, pp. 10726–10731, Jul. 2024.

[13] S. Joel, S. K. Yadav, and N. V. George, "Enhanced bias-compensated NLMS for adaptive DOA estimation," *IEEE Sensors Lett.*, vol. 8, no. 5, May 2024, Art. no. 6005004.

[14] P. Pal and P. P. Vaidyanathan, "Nested arrays: A novel approach to array processing with enhanced degrees of freedom," *IEEE Trans. Signal Process.*, vol. 58, no. 8, pp. 4167–4181, Aug. 2010.

[15] P. P. Vaidyanathan and P. Pal, "Sparse sensing with co-prime samplers and arrays," *IEEE Trans. Signal Process.*, vol. 59, no. 2, pp. 573–586, Feb. 2011.

[16] C. -L. Liu and P. P. Vaidyanathan, "Remarks on the spatial smoothing step in coarray MUSIC," *IEEE Signal Process. Lett.*, vol. 22, no. 9, pp. 1438–1442, Sep. 2015.

[17] Y. D. Zhang, M. G. Amin, and B. Himed, "Sparsity-based DOA estimation using co-prime arrays," in *Proc. IEEE Int. Conf. Acoust., Speech Signal Process.*, 2013, pp. 3967–3971.

[18] P. Pal and P. P. Vaidyanathan, "Correlation-aware techniques for sparse support recovery," in *Proc. IEEE Stat. Signal Process. Workshop*, 2012, pp. 53–56.

[19] O. Balkan, K. Kreutz-Delgado, and S. Makeig, "Localization of more sources than sensors via jointly-sparse Bayesian learning," *IEEE Signal Process. Lett.*, vol. 21, no. 2, pp. 131–134, Feb. 2014.

[20] S. Joel, S. K. Yadav, and N. V. George, "Coarray LMS: Adaptive underdetermined DOA estimation with increased degrees of freedom," *IEEE Signal Process. Lett.*, vol. 31, pp. 591–595, 2024.

[21] Y. Ma, X. Cao, and X. Wang, "Enhanced DOA estimation for MIMO radar in the case of limited snapshots," in *Proc. IEEE 11th Sensor Array Multichannel Signal Process. Workshop*, 2020, pp. 1–5.

[22] P. Pal and P. P. Vaidyanathan, "A grid-less approach to underdetermined direction of arrival estimation via low rank matrix denoising," *IEEE Signal Process. Lett.*, vol. 21, no. 6, pp. 737–741, Jun. 2014.

[23] C. Zhou, Y. Gu, X. Fan, Z. Shi, G. Mao, and Y. D. Zhang, "Direction-of-arrival estimation for coprime array via virtual array interpolation," *IEEE Trans. Signal Process.*, vol. 66, no. 22, pp. 5956–5971, Nov. 2018.

[24] Z. Yang, L. Xie, and C. Zhang, "A discretization-free sparse and parametric approach for linear array signal processing," *IEEE Trans. Signal Process.*, vol. 62, no. 19, pp. 4959–4973, Oct. 2014.

[25] E. J. Candès, X. Li, Y. Ma, and J. Wright, "Robust principal component analysis?," *J. ACM*, vol. 58, no. 3, pp. 1–37, 2011.